Systematic Assessment of the Photochemical Stability of Photoinitiator–Derived Macromolecular Chain Termini

ARTICLE *in* MACROMOLECULES · NOVEMBER 2015

Impact Factor: 5.8 · DOI: 10.1021/acs.macromol.5b02127

8 AUTHORS, INCLUDING:

David E Fast

Graz University of Technology

2 PUBLICATIONS **4** CITATIONS

SEE PROFILE

Anne Marie Kelterer

Graz University of Technology

46 PUBLICATIONS **498** CITATIONS

SEE PROFILE

Dmytro Neshchadin

Graz University of Technology

23 PUBLICATIONS **125** CITATIONS

SEE PROFILE

Georg Gescheidt

Graz University of Technology

166 PUBLICATIONS **1,667** CITATIONS

SEE PROFILE

Macromolecules

Article

pubs.acs.org/Macromolecules

Systematic Assessment of the Photochemical Stability of Photoinitiator-Derived Macromolecular Chain Termini

Andrea Lauer,[†,‡,#] David E. Fast,[§,#] Anne-Marie Kelterer,[§] Elena Frick,[†,‡] Dmytro Neshchadin,[§] Dominik Voll,[†,‡] Georg Gescheidt,[*,§] and Christopher Barner-Kowollik[*,†,‡]

[†]Preparative Macromolecular Chemistry, Institut für Technische Chemie und Polymerchemie, Karlsruhe Institute of Technology (KIT), Engesserstrasse 18, 76128 Karlsruhe, Germany

[‡]Institut für Biologische Grenzflächen (IBG), Karlsruhe Institute of Technology (KIT), Hermann-von-Helmholtz-Platz 1, 76344 Eggenstein-Leopoldshafen, Germany

[§]Institute of Physical and Theoretical Chemistry, NAWI Graz, Graz University of Technology, Stremayrgasse 9, 8010 Graz, Austria

Supporting Information

ABSTRACT: The photostability of polymeric materials is crucial for their applicability, especially under potentially harsh environmental conditions. In the current study, the influence of methyl-substitution on the photochemical stability of photoinitiator-derived benzoyl end groups is systematically investigated by a combination of pulsed-laser polymerization and subsequent size exclusion chromatography coupled with electrospray ionization mass spectrometry (PLP–SEC–ESI–MS), chemically induced dynamic nuclear polarization–nuclear magnetic resonance spectroscopy (CIDNP–NMR), and density functional theory (DFT) calculations. Poly(methyl methacrylate)s (pMMA) were synthesized employing benzoin-type photoinitiators with systematically substituted benzoyl moieties (i.e., 2-methylbenzoin, 3-methylbenzoin, 4-methylbenzoin, 2,4-dimethylbenzoin, 2,6-dimethylbenzoin, 2,4,6-trimethylbenzoin, 2,3,5,6-tetramethylbenzoin, and 2,3,4,5,6-pentamethylbenzoin). Photoinduced cleavage of the photoinitiator-based end group (irradiation at 351 and 355 nm) occurs solely for polymeric species with benzoyl end groups carrying no or only one *ortho*-methyl substituent/s, whereas all of the other substitution patterns lead to stable chain termini. The theoretical calculations suggest that the different reactivity can be traced back to shifts of the $n-\pi^*$ transitions by approximately +0.25 eV. The current investigation unambiguously evidences that methylation in both *ortho*-positions of the benzoin-type photoinitiator critically enhances the photostability of the resulting polymer chain termini providing a clear instruction for photoinitiator design leading to polymers with stable chain termini.

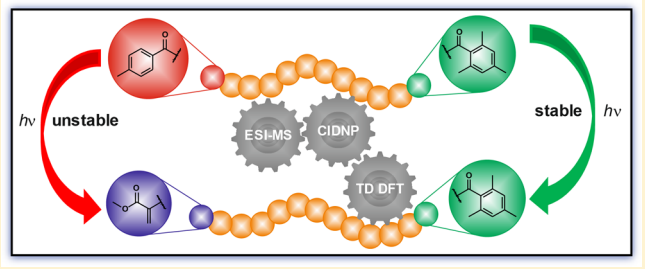

INTRODUCTION

Photoinduced radical polymerization has a wide variety of applications, including UV curing of coatings[1] and dental restorative materials,[2,3] fabrication of 3-dimensional objects[4] as well as adhesive technology.[5] Benzoin (2-hydroxy-2-phenylacetophenone) is a well-known type I photoinitiator which generates two radicals via α-cleavage upon irradiation (refer to Scheme 1). The resulting benzoyl (**A**) and benzyl alcohol radicals (**B**) initiate the polymerization of vinyl monomers and are incorporated as chain termini in the polymer.[6,7]

Scheme 1. Photocleavage of Benzoin leading to a Benzoyl Radical (A) and a Benzyl Alcohol Radical (B)

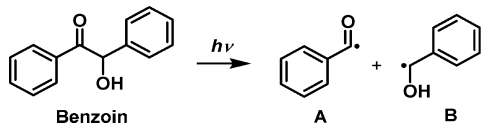

Despite the widespread use of radical photoinitiators, fundamental research regarding their basic photochemistry is still ongoing.[8−10] Most studies address the initial stages of photoinitiated polymerization, such as the excited state dynamics of photoinitiators,[11,12] initial radical reaction steps,[13,14] or addition rate constants to vinyl bonds.[15,16] In the current contribution, we focus on the photochemical reactivity of photoinitiator-derived end groups. Photostability of polymeric materials is crucial for their applicability under potentially harsh environmental conditions. In a previous study we have shown that benzoyl end groups present at poly(methyl methacrylate) (pMMA) termini can undergo photoinduced reactions at elevated irradiation energies.[17] In order to investigate the photochemically induced end group transformations, a combination of pulsed-laser polymerization (PLP) and subsequent size exclusion chromatography coupled with electrospray ionization mass spectrometry (SEC–ESI–MS), chemically induced dynamic nuclear polarization–nuclear

Received: September 27, 2015
Revised: October 30, 2015

DOI: 10.1021/acs.macromol.5b02127
Macromolecules XXXX, XXX, XXX–XXX

Scheme 2. Overall Research Strategy, Research Outcomes and Experimental Synergies for Photoinduced Reactions of Benzoyl-Terminated Poly(methyl methacrylate) via a Norrish Type I and II Pathway Followed in the Current Study

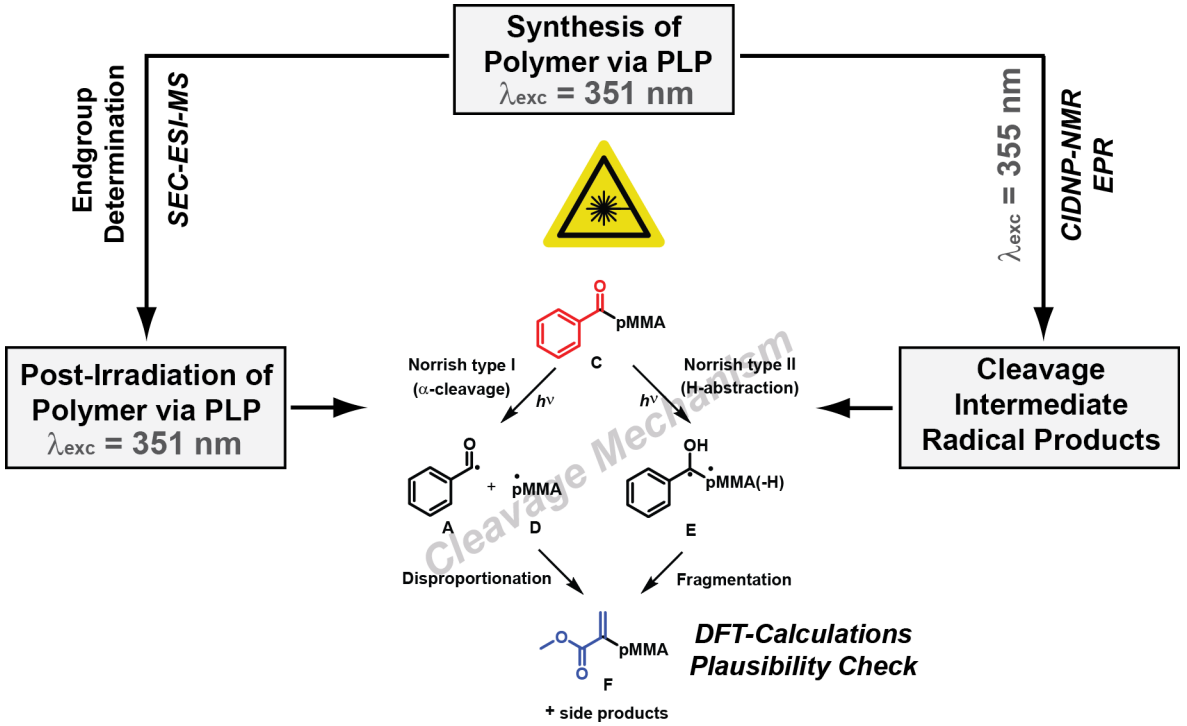

magnetic resonance spectroscopy (CIDNP−NMR), and density functional theory (DFT) calculations was employed. Upon laser-irradiation with high intensity, the benzoyl-terminated polymer (**C**) reacts via a Norrish type I (via **A**, **D**) or II (via **E**) pathway to form a polymeric species with an unsaturated end group (**F**, refer to Scheme 2).

On the basis of these results, we now present a systematic study on the influence of methyl-substitution on photochemical end group conversion. PLP−SEC−ESI−MS is a powerful tool for the analysis of polymeric materials[18−21] and was employed to determine the end group compositions of the polymers in the current investigation. PLP allows for finely adjusting the macromolecular chain length via tuning the laser frequency, which is crucial for the subsequent mass spectrometric analysis that is typically restricted to low intermediate molecular masses. In addition, PLP is an important technique for the determination of propagation rate coefficients.[22−24] In order to evidence the formation of double bonds during the photochemical end group conversion, hydrogenation experiments were carried out and the respective polymers were analyzed via SEC−ESI−MS, as well. Photo-CIDNP (chemically induced dynamic nuclear polarization) spectroscopy was employed in parallel to follow the mechanistic aspects of the end group conversion. It is a particularly suitable technique as only products formed from chemical reactions involving radical pairs are observed. CIDNP spectra display enhanced absorption and emission (or "polarized") NMR signals resulting from non-Boltzmann populations of magnetic energy levels.[25,26] Structural information regarding the reaction products can be deduced from the chemical shifts (δ) of the resonances. In addition, we performed density functional theory (DFT) calculations to theoretically rationalize our findings.

EXPERIMENTAL SECTION

Materials. Methyl methacrylate (MMA, Sigma-Aldrich, 99%, stabilized) was freed from inhibitor by passing through a column of activated basic alumina (VWR). Aluminum chloride (Acros Organics, anhydrous, 99%), 2-methylacetophenone (Alfa Aesar, anhydrous, 99.8%), 3-methylacetophenone (Sigma-Aldrich, 98%), 2,6-dimethylacetophenone (ABCR, 98%), benzene (anhydrous, Alfa Aesar, 99.8%), dioxane (Normapur, VWR), and selenium(IV) dioxide (ABCR, 99.8%) were used as received. 4-Methylbenzoin (**4-MB**, **1**), 2,4-dimethylbenzoin (**2,4-DMB**, **2**), 2,4,6-trimethylbenzoin (**TMB**, **3**), 2,3,5,6-tetramethylbenzoin (**TetMB**, **4**), and 2,3,4,5,6-pentamethylbenzoin (**PMB**, **5**), were synthesized according to literature procedures.[17] For the SEC−ESI−MS measurements, sodium iodide (Fluka, purris. p.a.), tetrahydrofuran (THF, Scharlau, multisolvent GPC grade, 250 ppm BHT), and methanol (VWR, chromanorm) were employed as received. For the postirradiation PLP experiments, methyl isobutyrate (MIB, Acros Organics, 99%) was used. Furthermore, *n*-hexane (VWR, p.a.) was used for precipitation of the synthesized pMMA. Pd on activated carbon (Pd/C, Acros Organics, unreduced, 5% Pd), hydrogen (H_2, Air Liquide, 99.999%) and a mixture of ethyl acetate (VWR, p.a.) /ethanol (technical grade, 95%) in a ratio of 1:1 v/v were used for the hydrogenation experiments as received. Acetonitrile-d_3 and chloroform-d_1 for NMR and CIDNP experiments were purchased from Sigma-Aldrich and used without additional treatment.

*Synthesis of 2-Oxo-2-o-tolylacetaldehyde (**6**), 2-Oxo-2-m-tolylacetaldehyde (**7**), and 2-(2,6-Dimethylphenyl)-2-oxoacetaldehyde (**8**).* The synthetic procedure was adapted from the literature[27] and is described exemplarily for 2-oxo-2-*o*-tolylacetaldehyde (**6**). To a solution of SeO_2 (8.29 g, 74.6 mmol, 1.00 equiv) in 2.3 mL water, 2-methylacetophenone (10.0 g, 74.6 mmol, 1.00 equiv) dissolved in 75 mL dioxane was added. The reaction mixture was refluxed for 6 h at 105 °C. Subsequently, the precipitated selenium was decanted and the solvent was evaporated under reduced pressure. Vacuum distillation gave **6** as a yellow oil (4.50 g, 41%) (**7**, yield = 44%; **8**, yield = 66%).

*Synthesis of 2-Hydroxy-2-phenyl-1-o-tolylethanone (2-Methylbenzoin, 2-MB, **9**), 2-Hydroxy-2-phenyl-1-m-tolylethanone (3-Methylbenzoin, 3-MB, **10**), and 1-(2,6-Dimethylphenyl)-2-hydroxy-2-phenylethan-1-one (2,6-Dimethylbenzoin, 2,6-DMB, **11**).* The synthetic procedure was adapted from the literature[28,29] and is

DOI: 10.1021/acs.macromol.5b02127
Macromolecules XXXX, XXX, XXX−XXX

described exemplarily for 2-methylbenzoin (**9**). Anhydrous aluminum chloride (8.10 g, 60.8 mmol, 2.00 equiv) was dissolved in 22 mL of anhydrous benzene. The suspension was cooled to 10 °C in an ice bath and 2-oxo-2-*o*-tolylacetaldehyde (4.50 g, 30.4 mmol, 1.00 equiv), dissolved in 22 mL of anhydrous benzene, was added dropwise to the suspension. The reaction was stirred for 2 h at 10 °C and subsequently the stirring was continued at ambient temperature overnight. The mixture was poured onto a mixture of ice/HCl_{conc}. The organic layer was separated and the aqueous phase was extracted twice with a minimal amount of benzene. The organic layers were combined and the solvent was removed under reduced pressure. The crude yellow-orange solid was divided into two equal parts. One part was purified by flash chromatography (cyclohexane:ethyl acetate, 3:1 v/v) and one part was recrystallized at 90 °C from ethanol. The two purified parts were combined to give **9** as an off-white powder (1.32 g, 19% yield) (**10**, yield = 10%; **11**, yield = 13%).

^{1}H NMR of **9** ($CDCl_3$, 400 MHz): δ 7.47 (d, ^3J = 7.7 Hz, 1H, $CH_{arom.}$), 7.24 (t, ^3J = 6.7 Hz, 1H, $CH_{arom.}$), 7.20–7.06 (m, 7H, $CH_{arom.}$), 5.81 (d, ^3J = 5.2 Hz, 1H, CHOH), 4.52 (d, ^3J = 5.8 Hz, 1H, CHO*H*), 2.19 (s, 3H, CH_3).

^{1}H NMR of **10** ($CDCl_3$, 400 MHz): δ 7.67 (s, 1H, $CH_{arom.}$), 7.60 (d, ^3J = 7.6 Hz, 1H, $CH_{arom.}$), 7.25–7.16 (m, 7H, $CH_{arom.}$), 5.87 (s, 1H, CHOH), 4.49 (s, 1H, CHO*H*), 2.26 (s, 3H, CH_3).

^{1}H NMR of **11** ($CDCl_3$, 400 MHz): δ 7.17–7.15 (m, 3H, $CH_{arom.}$), 7.12–7.08 (m, 1H, $CH_{arom.}$), 7.06–7.03 (m, 2H, $CH_{arom.}$), 6.87 (d, ^3J = 7.6 Hz, 2H, $CH_{arom.}$), 5.53 (d, ^3J = 5.3 Hz, 1H, CHOH), 4.40 (d, ^3J = 5.5 Hz, 1H, CHO*H*), 1.79 (s, 6H, CH_3).

Polymerization and Post-Irradiation of the Polymers. The PLP samples were all prepared with a concentration of $c_{Photoinitiator}$ = $5{\cdot}10^{-3}$ mol·L^{-1} in MMA (sample volume ~0.5 mL) and freed from oxygen by purging with nitrogen for 2 min. Subsequently, the samples were individually placed into the sample holder, which was held at the constant temperature of −2 °C by a thermostat (model: 1196D, VWR, Darmstadt, Germany). Polymerization and postirradiation of the polymer were carried out by an excimer laser system (Coherent XS-500, XeF, 351 nm, frequency variable from 1 to 500 Hz). The polymerizations were performed at a laser energy of 0.35 mJ/pulse (custom-build metal filter was implemented to reduce the laser energy) and the postirradiation of the polymer at 6 mJ/pulse at a frequency of 200 Hz with 90000 pulses. After the polymerization, the remaining monomer was evaporated and the polymer was purified by precipitation in *n*-hexane. For the post-irradiation, 15 mg of the respective polymer was dissolved in 0.5 mL of MIB, freed from oxygen by purging with nitrogen for 2 min and placed into the sample holder, which was held at a constant temperature of −2 °C. Afterward, the post-irradiated polymer was dried under air.

Hydrogenation of the Post-Irradiated Polymers. The hydrogenation reactions of the post-irradiated polymers were performed in a high pressure laboratory reactor (Berghof, BR-100) with a maximum operating pressure of 200 bar. The samples (**2-MB**, **3-MB**, **4-MB** and **2,4-DMB**) were prepared with 15 mg post-irradiated polymer and 3 mg Pd on activated carbon as the catalyst, diluted in a mixture of ethyl acetate /ethanol (1:1 v/v). The reactions were performed with a hydrogen pressure of 45 bar at ambient temperature for 4.5 h. After hydrogenation, the samples were filtered to remove the catalyst and the solvent was evaporated.

Size Exclusion Chromatography–Electrospray Ionization–Mass Spectrometry (SEC–ESI–MS). The spectra were recorded on a Q Exactive (Orbitrap) mass spectrometer (Thermo Fisher Scientific, San Jose, CA) equipped with an HESI II probe. The instrument was calibrated in the *m*/*z* range 74–1822 using premixed calibration solutions (Thermo Scientific). A constant spray voltage of 4.6 kV, a dimensionless sheath gas of 8, and a dimensionless auxiliary gas flow rate of 2 were applied. The capillary temperature and the S-lens RF level were set to 320 °C and 62.0, respectively. The Q Exactive was coupled to an UltiMate 3000 UHPLC System (Dionex, Sunnyvale, CA) consisting of a pump (LPG 3400SD), autosampler (WPS 3000TSL), and a thermostated column department (TCC 3000SD). Separation was performed on two mixed bed size exclusion chromatography columns (Polymer Laboratories, Mesopore 250 × 4.6 mm, particle diameter 3 μm) with precolumn (Mesopore 50 × 4.6 mm) operating at 30 °C. THF at a flow rate of 0.30 mL·min^{-1}

Scheme 3. Overview of the Investigated Photoinitiators

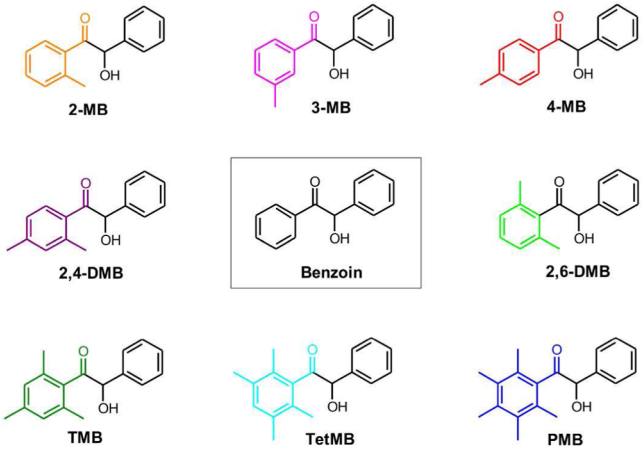

Scheme 4. Main Products of the Synthesis of 4-MB-Initiated pMMA at Low Laser Energies (0.35 mJ/pulse, 200 Hz) and Post-Irradiation at High Laser Energies (6 mJ/pulse, 200 Hz)

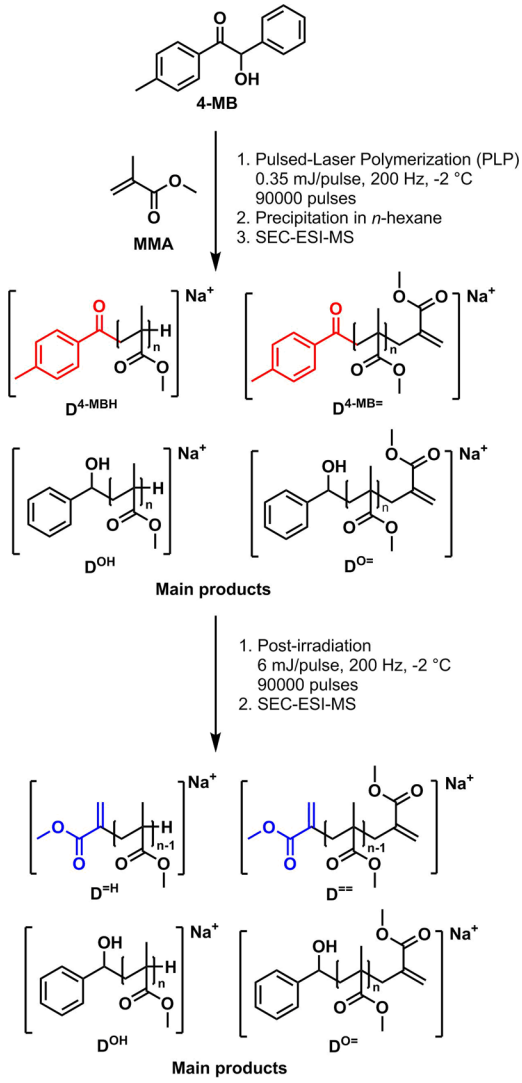

DOI: 10.1021/acs.macromol.5b02127
Macromolecules XXXX, XXX, XXX–XXX

Scheme 5. Disproportionation and Combination Products of the Polymer Initiated by 4-MB, at Low Laser Energies (0.35 mJ/pulse, 200 Hz), Post-Irradiated at High Laser Energies (6 mJ/pulse, 200 Hz) and Hydrogenation Experiments, as Detected by SEC−ESI−MS

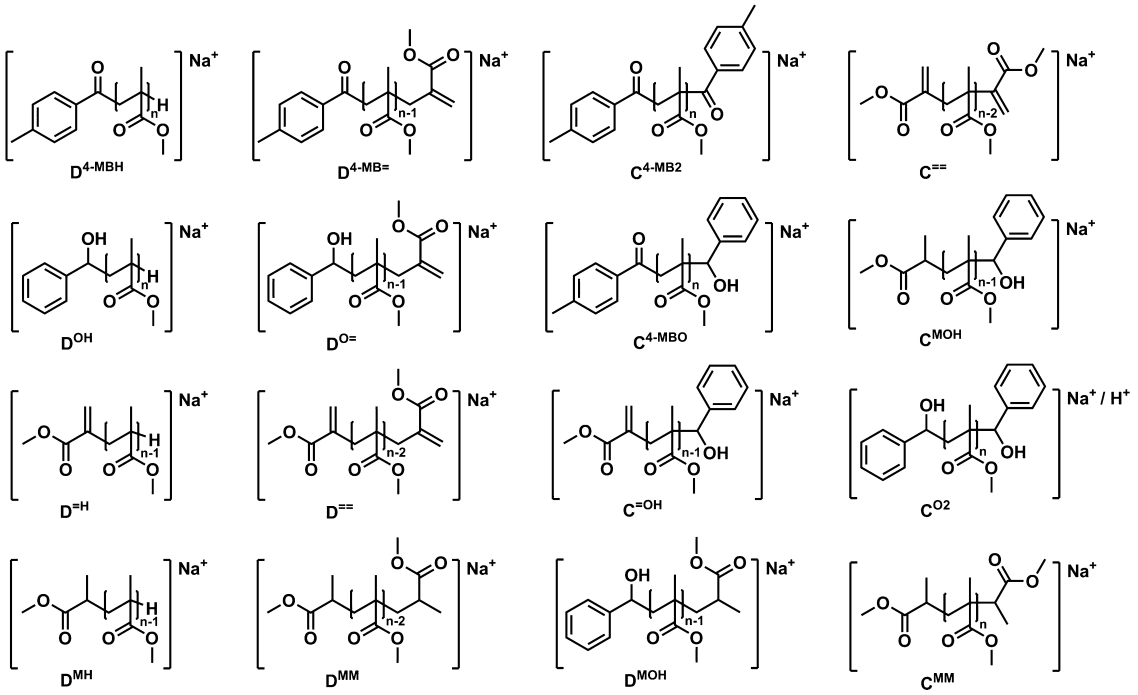

was used as eluent. The mass spectrometer was coupled to the column in parallel to a RI-detector (RefractoMax520, ERC, Japan) in a setup described earlier.[19] 0.27 mL·min^{-1} of the eluent were directed through the RI-detector and 30 μL·min^{-1} infused into the electrospray source after postcolumn addition of a 100 μM solution of sodium iodide in methanol at 20 μL·min^{-1} by a microflow HPLC syringe pump (Teledyne ISCO, Model 100DM). A 50 μL aliquot of a polymer solution with a concentration of 2 mg·mL^{-1} was injected into the HPLC system.

UV−Vis Spectroscopy. UV−Vis spectra of the photoinitiators were recorded on an Epoch 2 microplate spectrophotometer with Gen5 Data Analysis as software (refer to Figure S27). All measurements were carried out in methanol in a disposable plastic UV 96-well-plate with a thickness of 5 mm at ambient temperature. UV−Vis spectra of **4-MB**- and **TMB**-initiated pMMA were recorded on a Shimadzu UV-3101PC UV−Vis−NIR scanning spectrophotometer in acetonitrile.

^{1}H NMR. ^{1}H NMR spectra of the photoinitiators were recorded on a 400 MHz Bruker Ascend 400 spectrometer. All samples were dissolved in $CDCl_3$. Chemical shifts (δ) are referenced to the internal standard TMS (δ_H = 0 ppm).

^{1}H CIDNP. ^{1}H NMR and ^{1}H CIDNP spectra of the polymers were recorded on a 200 MHz Bruker AVANCE DPX spectrometer. Irradiation was carried out by using a frequency-tripled Quantel Brilliant B Nd:YAG laser (355 nm, ca. 80 mJ/pulse, 20 Hz, pulse duration 8 ns). A pulse sequence of "presaturation−laser flash−RF detection pulse (2 μs)−free induction decay" was used. Dummy CIDNP spectra without the application of a laser pulse were recorded to ensure an effective suppression of the parent NMR spectra. Chemical shifts (δ) are reported in ppm relative to tetramethylsilane (TMS) using the residual deuterated solvent signals as an internal reference (CD_3CN, δ_H = 1.94 ppm).

Computational Details. The S_0 singlet ground state and the T_1 triplet state were computed by DFT calculations (B3LYP)[30−33] with inclusion of Grimme's dispersion interaction correction D3.[34] The SVP basis set was used for this purpose.[35] Standard "tight" optimization criteria were applied. All minima were checked by frequency analysis to be true minima on the potential energy surface. Time-dependent DFT was used for the vertical excitations applying the CAM-B3LYP/TZVP[36,37] method. The optimization of the first singlet excited S_1 state was performed with TD-B3LYP-D3/SVP and the single point energies were recomputed by TD-CAM-B3LYP/TZVP for the S_0 and T_1. All computations were performed with the program *ORCA*.[38] Orbitals were depicted with *gabedit*[39] applying contour values of 0.05 au.

RESULTS AND DISCUSSION

In a previous study we have shown that an increasing number of methyl substituents on benzoin-type photoinitiators (PIs) leads to a decrease of the initiation ability of the resulting benzoyl radical fragments toward methyl methacrylate (MMA).[6] On the basis of these results we now systematically assess the influence of methyl-substitution on the photochemical reactivity of photoinitiator-derived benzoyl-type end groups. Thus, we synthesized various benzoin-type PIs, including three monomethyl-derivatives (2-, 3-, and 4-methylbenzoin, **2-MB**, **3-MB**, and **4-MB**, respectively) as well as two dimethyl-derivatives (2,4-, and 2,6-dimethylbenzoin, **2,4-DMB,** and **2,6-DMB**), 2,4,6-tri-, 2,3,5,6-tetra-, and 2,3,4,5,6-pentamethylbenzoin (**TMB**, **TetMB**, and **PMB**, respectively, refer to Scheme 3). This PI library is suitable to account for differences regarding steric and electronic−and thus photochemical−properties of the resulting polymer end groups and allows for the deduction of clear structure−property relationships.

Pulsed-Laser Polymerization and Post-Irradiation. The eight photoinitiators were employed to polymerize methyl methacrylate (**MMA**) in bulk via PLP at low laser energies (λ = 351 nm, 0.35 mJ/pulse, 200 Hz) to ensure intact end groups. The laser frequency of 200 Hz was selected to obtain relatively short polymer chains with different end groups, enabling their assessment by SEC−ESI−MS. The resulting polymers were precipitated in *n*-hexane to remove residual photoinitiator and post-irradiated at high laser energies

DOI: 10.1021/acs.macromol.5b02127
Macromolecules XXXX, XXX, XXX−XXX

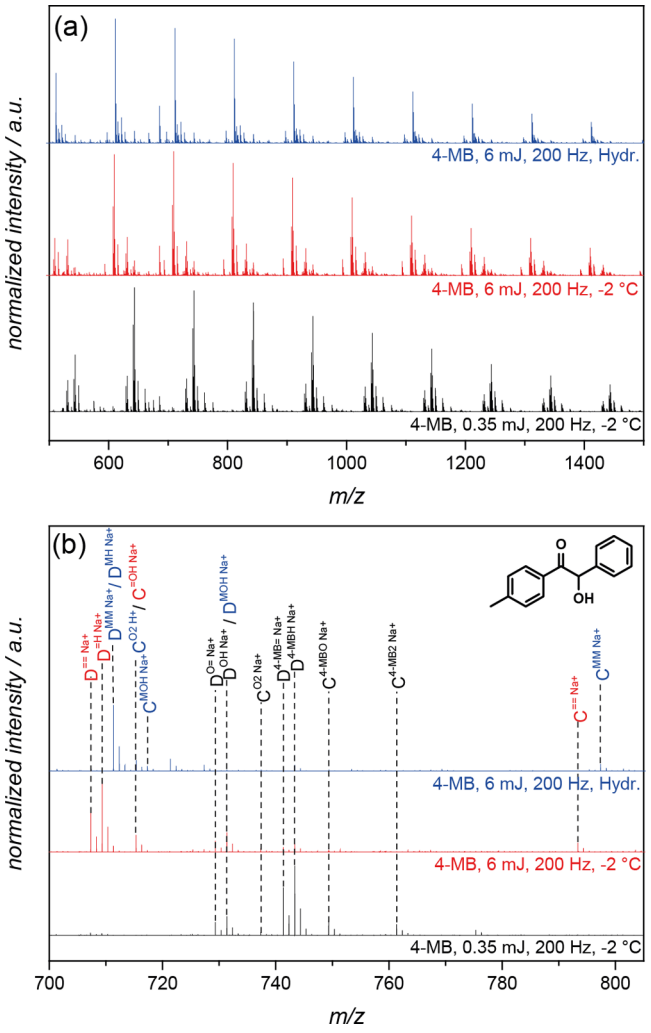

Figure 1. (a) SEC–ESI–MS overview spectra and (b) zoom into one repeat unit of the polymer initiated by **4-MB**, synthesized at low laser energies (0.35 mJ/pulse, 200 Hz, black spectrum), post-irradiated at higher laser energies (6 mJ/pulse, 200 Hz, red spectrum), and hydrogenated (blue spectrum).

(λ = 351 nm, 6 mJ/pulse, 200 Hz) in the nonpolymerizable solvent methyl isobutyrate (MIB) to trigger possible end group conversion of the chain termini resulting in the formation of double bonds. Scheme 4 illustrates the PLP and postirradiation conditions and the resulting main products on the example of **4-MB**.

SEC–ESI–MS. In the present study, the following nomenclature was adopted to label the observed ESI-MS signals. Disproportionation peaks occur in pairs with a mass difference of 2 amu. These peaks are labeled $\mathbf{D}^{\mathbf{XH}}$ or $\mathbf{D}^{\mathbf{X=}}$, where **X** defines the photoinitiator-derived end groups of the polymer chain in α-position, for instance **4-MB** for the 4-methylbenzoyl moiety. The end group in ω-position of the polymer chain is denoted as = (bearing a double bond) or **H** (bearing no double bond), depending on the role of the reactive site during the H-abstraction of the disproportionation process. Combination products are labeled with $\mathbf{C}^{\mathbf{X2}}$, $\mathbf{C}^{\mathbf{O2}}$, and $\mathbf{C}^{\mathbf{XO}}$, where **O** denotes the benzyl alcohol end groups and **2** denotes that the polymer is terminated with the same moiety on both ends. The disproportionation and combination products associated with the formation of new double bonds after post-irradiation and subsequent end group conversion are labeled with ==, =**H**, or =**XH**. After hydrogenation, these peaks shift by 4 and 2 amu, respectively, and are

Table 1. Overview of the Assigned Signals of the Polymers Synthesized at Low Laser Energies (0.35 mJ/pulse, 200 Hz), Post-Irradiated at High Laser Energies (6 mJ/pulse, 200 Hz) and Hydrogenation Experiments of 4-MB-Initiated pMMA, as Detected by SEC–ESI–MS with a Resolution of 77000

species	ionization	$(m/z)^{theo}$	$(m/z)^{exp}$	$\Delta(m/z)$
$\mathbf{D}^{==}$	Na^+	707.3255	707.3248	0.0007
$\mathbf{D}^{=H}$	Na^+	709.3411	709.3395	0.0016
$\mathbf{D}^{MM}$	Na^+	711.3568	711.3583	0.0015
$\mathbf{D}^{MH}$	Na^+	711.3568	711.3583	0.0015
$\mathbf{C}^{=OH}$	Na^+	715.3306	715.3315	0.0009
$\mathbf{C}^{O2}$	H^+	715.3694	715.3678	0.0016
$\mathbf{C}^{MOH}$	Na^+	717.3456	717.3473	0.0017
$\mathbf{D}^{O=}$	Na^+	729.3462	729.3453	0.0009
$\mathbf{D}^{OH}$	Na^+	731.3618	731.3604	0.0014
$\mathbf{D}^{MOH}$	Na^+	731.3619	731.3604	0.0015
$\mathbf{D}^{4\text{-}MB=}$	Na^+	741.3462	741.3453	0.0009
$\mathbf{D}^{4\text{-}MBH}$	Na^+	743.3618	743.3596	0.0022
$\mathbf{D}^{4\text{-}MBO}$	Na^+	749.3513	749.3497	0.0016
$\mathbf{C}^{O2}$	Na^+	737.3513	737.3505	0.0008
$\mathbf{D}^{4\text{-}MB2}$	Na^+	761.3513	761.3497	0.0016
$\mathbf{C}^{==}$	Na^+	793.3618	793.3613	0.0005
$\mathbf{C}^{MM}$	Na^+	797.3931	797.3951	0.0022

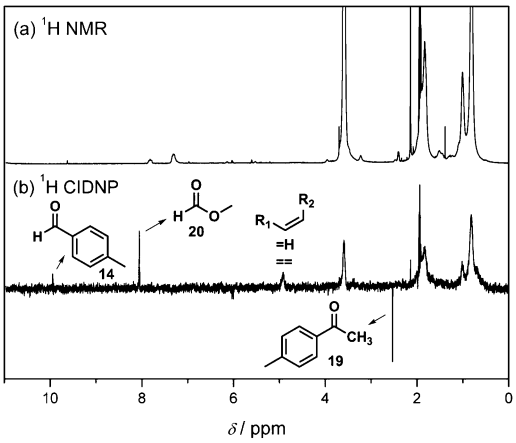

Figure 2. (a) ^{1}H NMR and (b) ^{1}H CIDNP spectrum of **4-MB**-pMMA synthesized at a laser energy of 0.35 mJ/pulse, recorded in CD_3CN at about 80 mJ/pulse with the assignment of the products formed from the radical reactions.

labeled with **MM** and **MH**, where **M** denotes an end group with a hydrogenated double bond. Scheme 5 depicts the polymeric combination and disproportionation products of **4-MB**-initiated pMMA (**4-MB**-pMMA) after the PLP, post-irradiation and hydrogenation experiments, as detected by SEC–ESI–MS.

Photochemically Unstable Chain Termini. First, we present our results for the **4-MB**-pMMA system upon irradiation at 351/355 nm as a representative example in detail (**2-MB**-, **3-MB**-, **4-MB**-, and **2,4-DMB**-pMMA, indicate matching reactivity patterns, therefore, we have collated their data in the Supporting Information). Figure 1a depicts the SEC–ESI–MS overview spectra of **4-MB**-pMMA synthesized at a laser energy of 0.35 mJ/pulse, 200 Hz (black spectrum), post-irradiated at a laser energy of 6 mJ/pulse, 200 Hz (red spectrum) and hydrogenated after post-irradiation (blue spectrum). A zoom into one repeat unit of the three polymer samples is displayed in Figure 1b and a complete assignment of the signals is listed in Table 1.

DOI: 10.1021/acs.macromol.5b02127
Macromolecules XXXX, XXX, XXX–XXX

Scheme 6. Photoinduced Reaction Pathways of 4-MB-Initiated pMMA (Synthesized at 0.35 mJ/Pulse, 200 Hz)

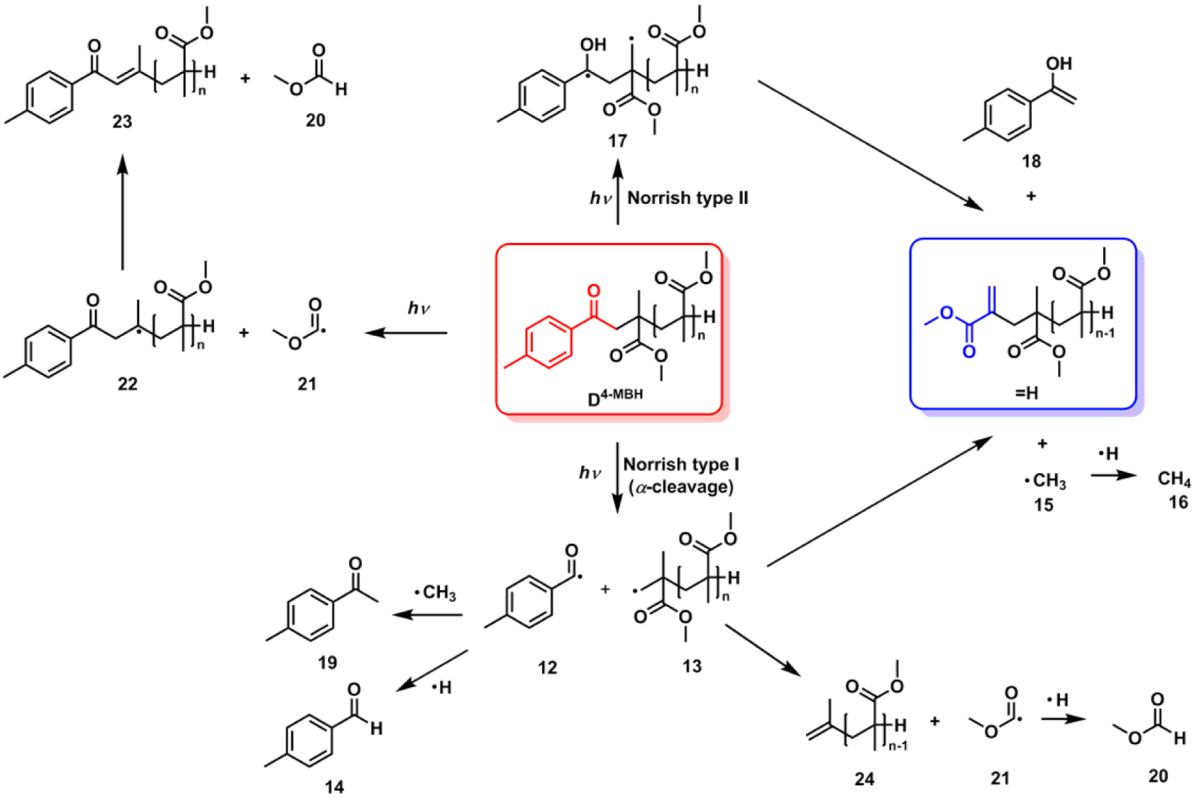

The mass spectrum of the polymer after PLP (0.35 mJ/pulse, 200 Hz, Figure 1b, black spectrum) shows the expected disproportionation ($\mathbf{D}^{\mathbf{4\text{-}MBH}}$, $\mathbf{D}^{\mathbf{4\text{-}MB=}}$, $\mathbf{D}^{\mathbf{OH}}$, $\mathbf{D}^{\mathbf{O=}}$, refer to Scheme 5) and combination products ($\mathbf{C}^{\mathbf{O2}}$, $\mathbf{C}^{\mathbf{4\text{-}MB2}}$, $\mathbf{C}^{\mathbf{4\text{-}MBO}}$, refer to Scheme 5). Post-irradiation of **4-MB**-pMMA (6 mJ/pulse, 200 Hz, Figure 1b, red spectrum) leads to the aforementioned end group conversion, indicated by the occurrence of signals at m/z = 707.3, 709.3, 715.3, and 793.4, which can be assigned to species $\mathbf{D}^{==}$, $\mathbf{D}^{=H}$, $\mathbf{C}^{=OH}$, and $\mathbf{C}^{==}$ (refer to Scheme 5), respectively. The formation of these species is accompanied by the nearly complete disappearance of the signals of $\mathbf{D}^{\mathbf{4\text{-}MB=}}$, $\mathbf{D}^{\mathbf{4\text{-}MBH}}$, $\mathbf{C}^{\mathbf{4\text{-}MBO}}$, and $\mathbf{C}^{\mathbf{4MB2}}$, indicating that the newly formed species originate from 4-methylbenzoyl-terminated polymer chains. Post-irradiated **4-MB**-pMMA was hydrogenated to further confirm the formation of polymeric species carrying double bonds at their chain termini. The signals of species $\mathbf{D}^{==}$ (m/z = 793.4) and $\mathbf{D}^{=H}$ (m/z = 709.3) show the expected shift of 4 and 2 amu, respectively, to m/z = 711.4 ($\mathbf{D}^{\mathbf{MM}}/\mathbf{D}^{\mathbf{MH}}$) in the mass spectrum of the hydrogenated polymer (Figure 1b, blue spectrum). Similarly, the signal of species $\mathbf{C}^{=OH}$ (m/z = 715.3) shifts to m/z = 717.3 ($\mathbf{C}^{\mathbf{MOH}}$) and the signal of species $\mathbf{C}^{==}$ (m/z = 793.4) shifts to m/z = 797.4 ($\mathbf{C}^{\mathbf{MM}}$). The signal at 715 amu stems from isobaric species $[\mathbf{C}^{\mathbf{O2}}]^{H+}$ and $[\mathbf{C}^{=OH}]^{Na+}$ (species with the same nominal mass). Analysis of the exact mass reveals that the signal in the mass spectrum of post-irradiated and hydrogenated **4-MB**-pMMA belongs to species $[\mathbf{C}^{\mathbf{O2}}]^{H+}$ (m/z = 715.3678) and is therefore unaffected by hydrogenation.

Figure 2 compares the ^{1}H NMR and ^{1}H CIDNP spectra (λ = 355 nm) of **4-MB**-pMMA (synthesized at a laser energy of 0.35 mJ/pulse, 200 Hz). The occurrence of polarized signals in the ^{1}H CIDNP spectrum (Figure 2b) reveals that the end group conversion proceeds via paramagnetic intermediates. According to our earlier findings for benzoyl-terminated polymer chains,[17] the 4-methylbenzoyl group can react via competing pathways (Norrish type I and II) as shown in Scheme 6.

The formation of 4-methylbenzoyl radicals **12** and polymer-derived radical **13** is in accordance with a Norrish type I reaction (α-cleavage). The singlet at δ = 9.9 ppm is characteristic of an aromatic aldehyde proton and can be assigned to 4-methylbenzaldehyde (**14**). It very likely originates from a hydrogen transfer reaction from **13** to the benzoyl radical **12**. The alkene **=H** can either be traced back to the disproportionation of **13** (possibly accompanied by the formation of methyl radicals **15**, and subsequently methane (**16**)) or to a Norrish type II reaction yielding 1,4-hydroxybiradical **17**. Fragmentation of biradical **17** leads to **=H** and enol **18**, which tautomerizes to 4-methylacetophenone (**19**). The singlet signal at δ = 2.5 ppm originates from the methyl-protons of acetophenone **19** accessible via both, Norrish type I and type II pathways (refer to Scheme 6). The absence of polarized signals of methane (**16**; δ = 0.2 ppm) suggests that the Norrish type II reaction is preferred in the case of 4-methylbenzoyl-terminated polymer chains. The weak polarized signals at δ = 4.8−5.0 ppm indicate the formation of new double bonds (= =, **=H**). The quartet at δ = 8.06 ppm (J = 0.8 Hz) derives from the single proton of methyl formate **20**. In line with our previous findings,[17] it can originate from **22** (direct cleavage of ester groups) or by a disproportionation reaction of radicals **13** (refer to Scheme 6).

In agreement with **4-MB**-pMMA, **3-MB**-pMMA shows polarized ^{1}H CIDNP signals (refer to Figure S20) indicating end group conversion yielding products corresponding to those displayed in Scheme 6. Similarly, the mass spectrum of post-irradiated **3-MB**-pMMA displays signals for species = = and **=H**, with hardly detectable signals of polymeric species with **3-MB**

DOI: 10.1021/acs.macromol.5b02127
Macromolecules XXXX, XXX, XXX−XXX

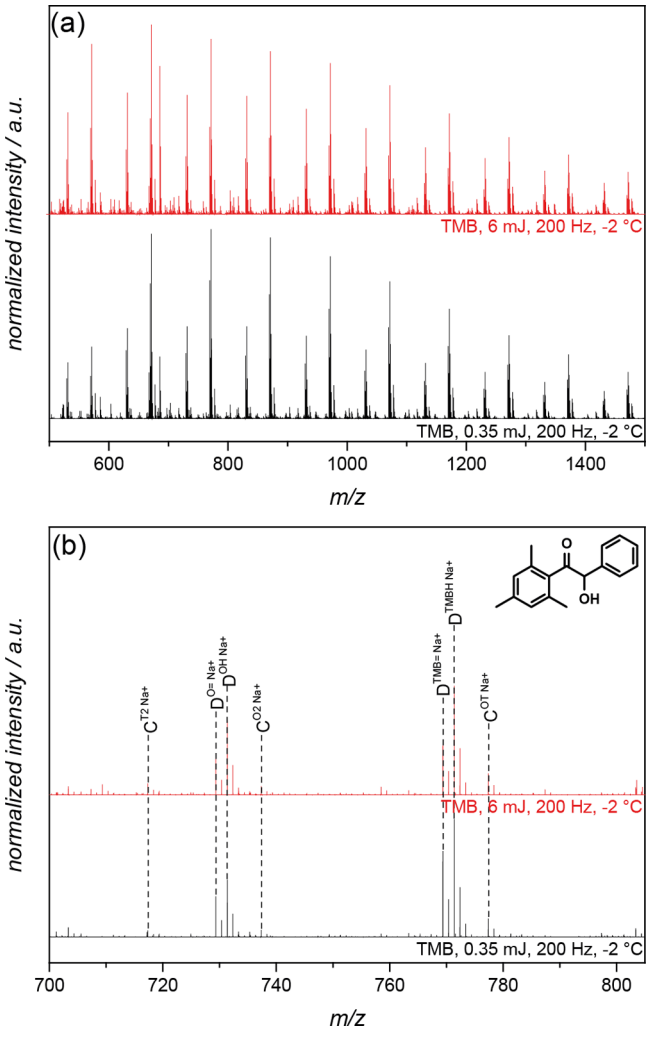

Figure 3. (a) SEC–ESI–MS overview spectrum and (b) zoom into one repeat unit of the polymer initiated by **TMB** at low laser energies (0.35 mJ, 200 Hz, black spectrum) and post-irradiated at higher laser energies (6 mJ, 200 Hz, red spectrum).

Table 2. Overview of the Assigned Signals of the Polymers Synthesized at Low Laser Energies (0.35 mJ/pulse, 200 Hz), Post-Irradiated at High Laser Energies (6 mJ/pulse, 200 Hz) of 4-MB-Initiated pMMA, as Detected by SEC–ESI–MS with a Resolution of 77000

species	ionization	$(m/z)^{theo}$	$(m/z)^{exp}$	$\Delta(m/z)$
$\mathbf{C}^{\mathbf{TMB2}}$	Na^+	717.3615	717.3598	0.0017
$\mathbf{D}^{\mathbf{OH}}$	Na^+	731.3618	731.3602	0.0016
$\mathbf{D}^{\mathbf{O=}}$	Na^+	729.3462	729.3449	0.0013
$\mathbf{C}^{\mathbf{O2}}$	Na^+	737.3513	737.3495	0.0018
$\mathbf{D}^{\mathbf{TMB=}}$	Na^+	769.3775	769.3763	0.0012
$\mathbf{D}^{\mathbf{TMBH}}$	Na^+	771.3931	771.3915	0.0016
$\mathbf{C}^{\mathbf{TMBO}}$	Na^+	777.3826	777.3812	0.0014

end groups (refer to Figure S13). SEC–ESI–MS analysis of post-irradiated **2-MB**- and **2,4-DMB**-pMMA revealed partial end group conversion (refer to Figures S12 and S9), which can be illustrated by a slight decrease of the benzoyl moieties signals (e.g., $\mathbf{D}^{\mathbf{2\text{-}MBH}}$, $\mathbf{D}^{\mathbf{2\text{-}MB=}}$) and the lack of the cleavage and hydrogenation signals of the combination products ($\mathbf{C}^{==}$ and $\mathbf{C}^{\mathbf{MM}}$). However, no ^{1}H CIDNP effects could be established, pointing to a low efficiency of the photochemical end group conversion reaction owing to the lower overall energy input and sensitivity of the CIDNP measurements compared to ESI–MS. To clearly demonstrate the partial end group conversion of **2-MB**- and **2,4-DMB**-pMMA, a quantitative comparison of the decomposition peaks with the initiation peaks for the initiators **2-MB** and **2,4-DMB**, **3-MB**, and **4-MB** was carried out. Therefore, the heights (Δh) of each first peak of every repeating unit's respective disproportionation peak clusters (for example **2-MB=** and = =, refer to Figure S22) were compared with each other. Specifically the peak height Δh^{Dx} was employed for the calculation of the mole fraction $F^x(i)$, whereas X defines the respective end group of the initiating or decomposition fragment. For further equations or details see literature.[40,41] A plot of the $F^x(i)$ values for each fragment X against the degree of polymerization DP_n (refer to Figure S23–S26) exhibits a constant gradient close to zero, if a chain length independent ESI process takes place. However, this only applies when the compared end groups are relatively similar to each other. In our case the end groups were structurally different due to the fact that one end group is bearing an aromatic system and the other end group only free double bonds. The $F^x(i)$ plots of **2-MB**, **2,4-DMB**, **3-MB**, and **4-MB** showed an asymptotic behavior originating from the different ionization abilities of the end groups. With increasing DP_n, the mole fractions of the initiating end groups ($F^{2\text{-}MB=}(i)$) increase and those of the decomposition end groups decrease ($F^{==}(i)$), which is associated with the increasing dependence of longer chains toward ionization effects resulting from the respective chain termini. Thus, a quantitative picture of the decomposition signals can be assumed for long chains, i.e., high DP_n values. To keep the comparison simple, **2-MB** and **2,4-DMB** were compared against **3-MB** and **4-MB**, due to their similar decomposition behavior. **2-MB** and **2,4-DMB** showed an 8-fold weaker cleavage behavior compared to **3-MB** and **4-MB**, which is arguably the reason for the lack of cleavage signals in the CIDNP spectrum for **2-MB** and **2,4-DMB**.

The occurrence of photoinduced reactions for **2-MB**-, **3-MB**-, **4-MB**-, and **2,4-DMB**-pMMA evidence that the respective chain termini are photochemically unstable under our experimental conditions. Such a behavior can be traced back to the methyl-substitution pattern (no or only one *ortho*-position of the benzoyl moiety carries a methyl group, refer to the DFT calculations section below).

Photochemically Stable Chain Termini. Here, we present our results with respect to the behavior of 2,4,6-trimethylbenzoin-initiated pMMA (**TMB**-pMMA) upon irradiation at 351/355 nm as a representative example of a photochemically stable chain terminus in a detailed fashion (**2,6-DMB**-, **TetMB**-, and **PMB**-pMMA indicate similar reactivity patterns, therefore, we have summarized their data in the Supporting Information). Figure 3a depicts the SEC–ESI–MS overview spectra of **TMB**-pMMA synthesized at a laser energy of 0.35 mJ/pulse, 200 Hz (black spectrum) and post-irradiated at a laser energy of 6 mJ/pulse 200 Hz (red spectrum). A zoom into one repeat unit of the two polymer samples is displayed in Figure 3b and a complete assignment of the signals is listed in Table 2.

The mass spectrum of the polymer after PLP (0.35 mJ/pulse, 200 Hz, Figure 3b, black spectrum) shows the expected disproportionation ($\mathbf{D}^{\mathbf{TMBH}}$, $\mathbf{D}^{\mathbf{TMB=}}$, $\mathbf{D}^{\mathbf{OH}}$, $\mathbf{D}^{\mathbf{O=}}$, refer to Scheme 7) and combination products ($\mathbf{C}^{\mathbf{O2}}$, $\mathbf{C}^{\mathbf{TMB2}}$, $\mathbf{C}^{\mathbf{TMBO}}$, refer to Scheme 7). Post-irradiated **TMB**-pMMA (6 mJ/pulse, 200 Hz) shows no changes in the mass spectrum (Figure 3b, red spectrum), thus evidencing the 2,4,6-trimethyl-substituted

DOI: 10.1021/acs.macromol.5b02127
Macromolecules XXXX, XXX, XXX–XXX

Scheme 7. Disproportionation and Combination Products of the Polymer Initiated by TMB, at Low Laser Energies (0.35 mJ/pulse, 200 Hz), Post-Irradiated at Higher Laser Energies (6 mJ/pulse, 200 Hz), as Detected by SEC−ESI−MS

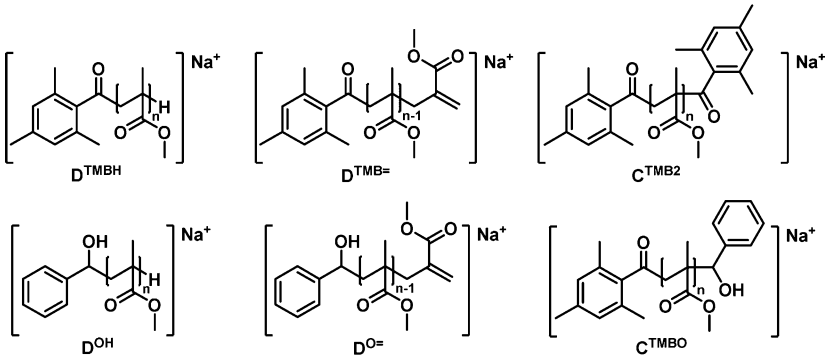

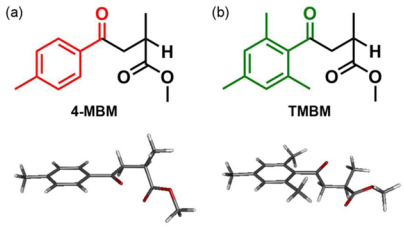

Figure 4. Structures and optimized geometries of polymer model compounds (a) **4-MBM** and (b) **TMBM**. Optimization: DFT/B3LYP-D3/SVP.[30−35]

benzoyl end group (**TMB**) to be photochemically stable under our experimental conditions.

In agreement with the ESI-MS measurements, the ^{1}H CIDNP spectrum of **TMB**-pMMA (synthesized at a laser energy of 0.35 mJ/pulse, 200 Hz) shows no polarized NMR signals (Figure S16), indicating that no photoinduced radical reactions occur at the chain terminus. Similarly, no polarized signals in CIDNP and no changes in the SEC−ESI−MS spectra after post-irradiation (at a laser energy of 6 mJ/pulse, 200 Hz) were observed for **2,6-DMB**-, **TetMB**-, and **PMB**-initiated pMMA (refer to Supporting Information).

DFT Calculations. The experimental results discussed above unambiguously demonstrate that polymers carrying **2,6-DMB**, **TMB**, **TetMB**, and **PMB** end groups are particularly inert to irradiation at 351 and 355 nm. The common feature of these end groups is the methyl-substitution in both *ortho*-positions of the benzoyl moiety. We have performed density functional theory (DFT) calculations of polymer model compounds to obtain further insights into the reactivity of the differently end-capped polymers. The model species consist of the methyl-substituted benzoyl moiety connected to one methyl methacrylate (**M**) unit. Additionally, we have calculated models with three monomer units, however, in terms of the excited states, no significant differences were present between the two approaches. Consequently, we only focus on the models with one monomer unit. In analogy to the experimental results we discuss two model compounds exemplarily: the 4-methyl- (**4-MBM**) and 2,4,6-trimethyl-substituted model (**TMBM**). The structures and minimized geometries are depicted in Figure 4. In **4-MBM**, the methyl-substituted phenyl ring is coplanar with the carbonyl group whereas it is twisted out of plane with a dihedral angle of ca. 70° vs. the carbonyl group in **TMBM**.

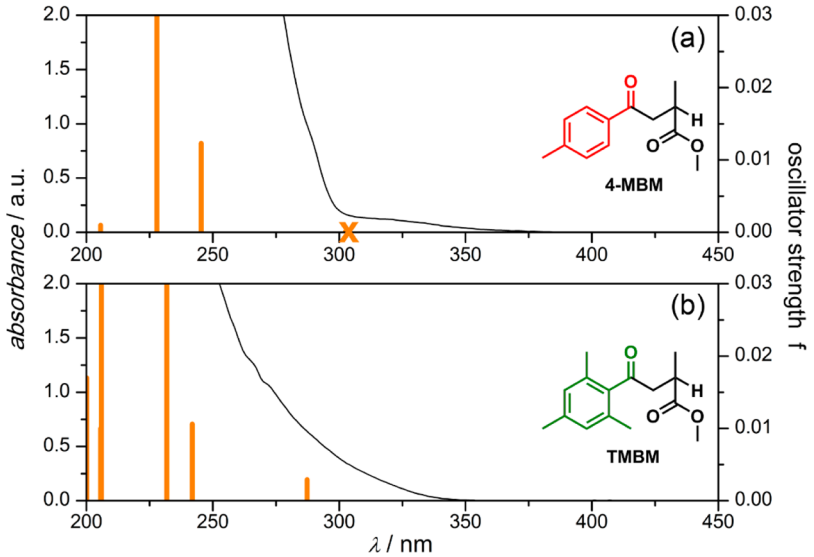

Figure 5. Experimental absorption spectra of (a) **4-MB**-pMMA and (b) **TMB**-pMMA in acetonitrile solution (black) and calculated singlet excitations (orange) of the corresponding model compounds **4-MBM** (S_1 is marked with an ×) and **TMBM**. Calculated at the TD-DFT/CAM-B3LYP/TZVP[36,37] level of theory.

DOI: 10.1021/acs.macromol.5b02127
Macromolecules XXXX, XXX, XXX−XXX

Scheme 8. Overview of the Investigated Polymers with Differently Methylated Benzoyl End Groups and Their Behavior under Post-Irradiation (λ = 351 nm, 6 mJ/pulse) and CIDNP Conditions (λ = 351 nm)[a]

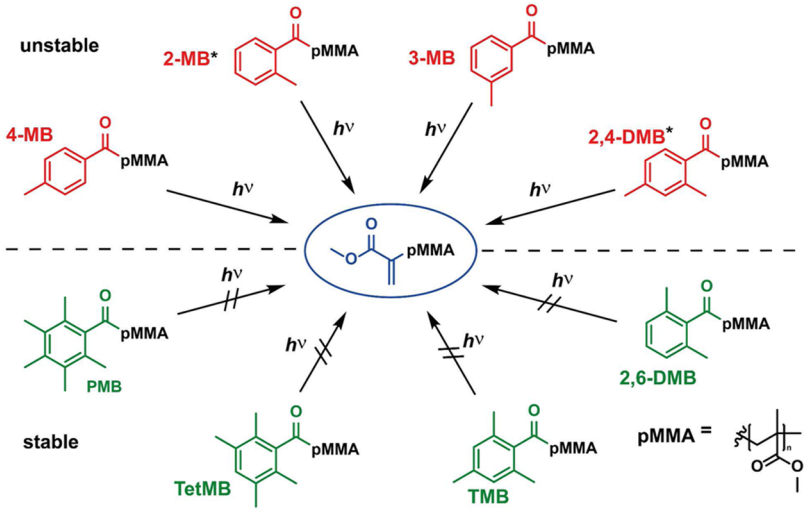

[a]Photoinitiator-derived chain termini depicted in red undergo photoinduced end group conversion, whereas chain termini depicted in green are stable. For end groups marked with an asterisk, photoinduced reactions were only observed via post-irradiation and subsequent SEC–ESI–MS analysis.

On the basis of the minimized geometries, (vertical) singlet excitations were computed. Figure 5 shows the experimental absorption spectra of **4-MB**- and **TMB**-pMMA (synthesized at a laser energy of 0.35 mJ/pulse, 200 Hz) in acetonitrile (black) jointly with the calculated ones (orange). The agreement between the experimental spectra and the calculations is reasonable in view of the CAM-B3LYP method, which has been shown to overestimate vertical transition energies by ca. 0.5 eV.[42] Accordingly, the computed 303 nm (4.1 eV, **4-MBM**) and 287 nm (4.3 eV, **TMBM**) for the S_1 transitions correspond to excitations with 345 nm (3.6 eV) and 317 nm (3.9 eV), respectively, in the experiment.

Owing to coplanarity between the carbonyl and the phenyl moiety, the π-system is more delocalized in **4-MBM** than in **TMBM**, leading to distinct differences in the absorptions. For **4-MBM**, the S_1 singlet excitation at 303 nm (marked with 'x' in Figure 5a) is assigned as $n-\pi^*$ transition from the carbonyl oxygen lone pair into the π-system. In the case of **TMBM** the transition is blue-shifted to 287 nm (refer to Figure 5b). The oscillator strength (0.0029) of this $n-\pi^*$ transition is higher than in **4-MBM** (0.0001) due to differing orbital characters (refer to Table S3). According to El-Sayed's rule,[43] $n-\pi^*$ states can easily undergo intersystem crossing (ISC) into $\pi-\pi^*$ triplet states, which undergo Norrish type I or II reactions. For both model compounds $\pi-\pi^*$ triplet states were computed, yet due to the blue-shifted S_1 singlet excitation of **TMBM** (287 nm), we conclude that only **4-MB**-terminated polymer chains can be excited into the S_1 under our experimental conditions (λ = 351 nm for post-irradiation and λ = 355 nm for CIDNP experiments). ISC into the triplet state and subsequent Norrish type I or II reactions leads to the experimentally observed formation of polymeric species with an unsaturated end group. In analogy to **4-MBM**, model compounds **2-MBM**, **3-MBM** and **2,4-DMBM** have $n-\pi^*$ transitions in the range of 305 to 309 nm (refer to Table S4). $n-\pi^*$ transitions of model compounds **2,6-DMBM**, **TetMBM** and **PMBM** are in the range of 283 to 288 nm (refer to Table S4) and can therefore not be excited into the S_1 state under our experimental conditions.

CONCLUSIONS

We synthesized a library of pMMAs via PLP (at a laser energy of 0.35 mJ/pulse, 200 Hz) employing eight benzoin-type photoinitiators with differently methylated benzoyl moieties. The photochemical stability of the resulting polymers with substituted benzoyl end groups was investigated by a combination of post-irradiation (λ = 351 nm, 6 mJ/pulse, 200 Hz) and subsequent SEC–ESI–MS analysis as well as photo-CIDNP spectroscopy (λ = 355 nm). Photoinduced end group transformations were solely observed for polymeric species with benzoyl end groups carrying no or only one *ortho*-methyl substituent/s (**2-MB**, **3-MB**, **4-MB**, and **2,4-DMB**—referred to as "photochemically unstable"—refer to Scheme 8). SEC–ESI–MS spectra of the post-irradiated polymers revealed the formation of new polymeric species with unsaturated end groups. The end group conversion proceeds via Norrish type I and II reaction pathways as we have evidenced by photo-CIDNP spectroscopy. Polymers containing benzoyl end groups with methyl-substitution in both *ortho*-positions were stable under post-irradiation and CIDNP conditions (**2,6-DMB**, **TMB**, **TetMB**, and **PMB**—referred to as "photochemically stable"—refer to Scheme 8).

DFT calculations for polymer model compounds (consisting of the methyl-substituted benzoyl end group and one methyl methacrylate unit) suggest that the differences in reactivity can be traced back to a systematic shift of the $n-\pi^*$ transitions (S_1 singlet excitations). Photochemically unstable end groups are characterized by a coplanarity of the substituted phenyl moiety and the carbonyl group, leading to $n-\pi^*$ transitions in the range of 303 to 309 nm. Photoexcitation and ISC into the $\pi-\pi^*$ triplet state, which undergoes a Norrish type I or II reaction, leads to the formation of the experimentally observed polymeric species with an unsaturated end group. The substituted phenyl moiety of photochemically stable end groups is twisted out of plane vs. the carbonyl group, leading to differing electronic properties and thus to blue-shifted $n-\pi^*$ transitions in the range of 283 to 288 nm. Thus, we conclude that post-irradiation of these end-capped polymers at 351/355 nm is

DOI: 10.1021/acs.macromol.5b02127
Macromolecules XXXX, XXX, XXX–XXX

inefficient in producing $n-\pi^*$ transitions, therefore rendering them photochemically stable.

Our observations suggest that simple methyl-substitution of benzoin-type photoinitiators leads to enhanced photochemical stability of the resulting polymer end groups. Methylation in both *ortho*-positions of the benzoyl chain termini results in a blue-shift of the $n-\pi^*$ transition, thus the respective polymer chains are potentially less prone to photodegredation under environmental conditions such as solar irradiation.

■ ASSOCIATED CONTENT

Supporting Information

The Supporting Information is available free of charge on the ACS Publications website at DOI: 10.1021/acs.macromol.5b02127.

^{1}H NMR and SEC−ESI−MS spectra of **2**, **4**, **5**, **9**, **10**, and **11**; ^{1}H NMR spectra of **1** and **3**, $F^x(i)$ plots of **1**, **2**, **9**, and, **10**; SEC−ESI−MS spectrum of **9** for the peak height evaluation; CIDNP−NMR data for polymers initiated by **2**, **3**, **4**, **5**, **9**, **10**, and **11**; and DFT data, including the first five vertical excitations and the relevant molecular orbitals for **4-MBM** and **TMBM**, the molecular orbitals of S_1 and T_1 for **4-MBM** and **TMBM**, and the S_1 singlet excitations for all calculated model compounds (PDF)

■ AUTHOR INFORMATION

Corresponding Authors

*(C.B.-K.) E-mail: christopher.barner-kowollik@kit.edu.
*(G.G.) E-mail: g.gescheidt-demner@tugraz.at.

Author Contributions

#These authors contributed equally.

Notes

The authors declare no competing financial interest.

■ ACKNOWLEDGMENTS

C.B.-K. acknowledges financial support for the current project from the German Research Council (DFG) as well as long term funding from the Karlsruhe Institute of Technology (KIT) in the context of the STN program of the Helmholtz association. G.G. acknowledges financial support for the current project from the Austrian Science Fund (FWF, project-no.: I 1614) as well as support by NAWI Graz.

■ REFERENCES

(1) Allen, N. S. *J. Photochem. Photobiol., A* **1996**, *100*, 101.
(2) Ahn, D.; Sathe, S. S.; Clarkson, B. H.; Scott, T. F. *Dent. Mater.* **2015**, *31*, 1075.
(3) Anseth, K. S.; Newman, S. M.; Bowman, C. N. In *Biopolymers II*; Peppas, N. A., Langer, R. S., Eds.; Springer: Berlin and Heidelberg, Germany, 1995; Vol. *122*, p. 177.
(4) Sun, H. B.; Kawata, S. *Adv. Polym. Sci.* **2004**, *170*, 169.
(5) Allen, N. S. *Photochemistry* **1996**, *27*, 303.
(6) Voll, D.; Hufendiek, A.; Junkers, T.; Barner-Kowollik, C. *Macromol. Rapid Commun.* **2012**, *33*, 47.
(7) Voll, D.; Junkers, T.; Barner-Kowollik, C. *Macromolecules* **2011**, *44*, 2542.
(8) Frick, E.; Ernst, H. A.; Voll, D.; Wolf, T. J. A.; Unterreiner, A.-N.; Barner-Kowollik, C. *Polym. Chem.* **2014**, *5*, 5053.
(9) Jockusch, S.; Turro, N. J. *J. Am. Chem. Soc.* **1998**, *120*, 11773.
(10) Sabol, D.; Gleeson, M. R.; Liu, S.; Sheridan, J. T. *J. Appl. Phys.* **2010**, *107*, 053113.
(11) Wolf, T. J. A.; Voll, D.; Barner-Kowollik, C.; Unterreiner, A.-N. *Macromolecules* **2012**, *45*, 2257.
(12) Jockusch, S.; Landis, M. S.; Freiermuth, B.; Turro, N. J. *Macromolecules* **2001**, *34*, 1619.
(13) Griesser, M.; Neshchadin, D.; Dietliker, K.; Moszner, N.; Liska, R.; Gescheidt, G. *Angew. Chem. Int. Ed.* **2009**, *48*, 9359.
(14) Weber, M.; Turro, N. J.; Beckert, D. *Phys. Chem. Chem. Phys.* **2002**, *4*, 168.
(15) Colley, C. S.; Grills, D. C.; Besley, N. A.; Jockusch, S.; Matousek, P.; Parker, A. W.; Towrie, M.; Turro, N. J.; Gill, P. M. W.; George, M. W. *J. Am. Chem. Soc.* **2002**, *124*, 14952.
(16) Hristova, D.; Gatlik, I.; Rist, G.; Dietliker, K.; Wolf, J.-P.; Birbaum, J.-L.; Savitsky, A.; Möbius, K.; Gescheidt, G. *Macromolecules* **2005**, *38*, 7714.
(17) Voll, D.; Neshchadin, D.; Hiltebrandt, K.; Gescheidt, G.; Barner-Kowollik, C. *Macromolecules* **2012**, *45*, 5850.
(18) Aaserud, D. J.; Prokai, L.; Simonsick, W. J. *Anal. Chem.* **1999**, *71*, 4793.
(19) Gruendling, T.; Guilhaus, M.; Barner-Kowollik, C. *Macromolecules* **2009**, *42*, 6366.
(20) Nielen, M. W. F. *Rapid Commun. Mass Spectrom.* **1996**, *10*, 1652.
(21) Voll, D.; Junkers, T.; Barner-Kowollik, C. *J. Polym. Sci., Part A: Polym. Chem.* **2012**, *50*, 2739.
(22) Barner-Kowollik, C.; Bennet, F.; Schneider-Baumann, M.; Voll, D.; Rölle, T.; Fäcke, T.; Weiser, M.-S.; Bruder, F.-K.; Junkers, T. *Polym. Chem.* **2010**, *1*, 470.
(23) Kockler, K. B.; Haehnel, A. P.; Fleischhaker, F.; Schneider-Baumann, M.; Misske, A. M.; Barner-Kowollik, C. *Macromol. Chem. Phys.* **2015**, *216*, 1573.
(24) Haehnel, A. P.; Schneider-Baumann, M.; Arens, L.; Misske, A. M.; Fleischhaker, F.; Barner-Kowollik, C. *Macromolecules* **2014**, *47*, 3483.
(25) Goez, M. *Annu. Rep. NMR Spectrosc.* **2009**, *66*, 77.
(26) Yurkovskaya, A.; Morozova, O.; Gescheidt, G. Structures and Reactivity of Radicals Followed by Magnetic Resonance. In *Encyclopedia of Radicals in Chemistry, Biology and Materials*; Chatgilialoglu, C., Studer, A., Eds.; John Wiley & Sons, Ltd: Chichester, U.K., 2012.
(27) Gray, A. R.; Fuson, R. C. *J. Am. Chem. Soc.* **1934**, *56*, 739.
(28) Weinstock, H. H.; Fuson, R. C. *J. Am. Chem. Soc.* **1936**, *58*, 1986.
(29) Fuson, R. C.; Weinstock, H. H.; Ullyot, G. E. *J. Am. Chem. Soc.* **1935**, *57*, 1803.
(30) Becke, A. D. *J. Chem. Phys.* **1993**, *98*, 5648.
(31) Lee, C.; Yang, W.; Parr, R. G. *Phys. Rev. B: Condens. Matter Mater. Phys.* **1988**, *37*, 785.
(32) Stephens, P. J.; Devlin, F. J.; Chabalowski, C. F.; Frisch, M. J. *J. Phys. Chem.* **1994**, *98*, 11623.
(33) Vosko, S. H.; Wilk, L.; Nusair, M. *Can. J. Phys.* **1980**, *58*, 1200.
(34) Grimme, S.; Antony, J.; Ehrlich, S.; Krieg, H. *J. Chem. Phys.* **2010**, *132*, 154104.
(35) Schäfer, A.; Horn, H.; Ahlrichs, R. *J. Chem. Phys.* **1992**, *97*, 2571.
(36) Schäfer, A.; Huber, C.; Ahlrichs, R. *J. Chem. Phys.* **1994**, *100*, 5829.
(37) Yanai, T.; Tew, D. P.; Handy, N. C. *Chem. Phys. Lett.* **2004**, *393*, 51.
(38) Neese, F. *Wiley Interdisciplinary Reviews: Computational Molecular Science* **2012**, *2*, 73.
(39) Allouche, A.-R. *J. Comput. Chem.* **2011**, *32*, 174.
(40) Buback, M.; Günzler, F.; Russell, G. T.; Vana, P. *Macromolecules* **2009**, *42*, 652.
(41) Günzler, F. Ph.D. Thesis, University of Göttingen, 2008.
(42) Kelterer, A.-M.; Uray, G.; Fabian, W. M. F. *J. Mol. Model.* **2014**, *20*, 2217.
(43) El-Sayed, M. A. *J. Chem. Phys.* **1963**, *38*, 2834.

DOI: 10.1021/acs.macromol.5b02127
Macromolecules XXXX, XXX, XXX−XXX